Environ. Sci. Technol. **1999**, *33,* 730−736

Counter-Diffusion of Isotopically Labeled Trichloroethylene in Silica Gel and Geosorbent Micropores: Column Results

CHARLES J. WERTH*,† AND MARTIN REINHARD

Environmental Engineering and Science, Department of Civil and Environmental Engineering, Stanford University, Stanford, California 94305-4020

To investigate counter-diffusion in microporous sorbents, the rate of exchange between deuterated trichloroethylene (DTCE) in fast desorbing sites and nondeuterated TCE (^{1}HTCE) in slow desorbing sites was measured. Exchange rates were measured for a silica gel, a Santa Clara sediment, and a Livermore clay/silt fraction, all at 100% relative humidity and 30 °C. Initially, solids were packed into stainless steel columns and incubated with ^{1}HTCE for 1−3 weeks. After incubation, ^{1}HTCE was replaced with DTCE in fast desorbing sites. Next, columns were capped (i.e., sealed), and DTCE was allowed to exchange with ^{1}HTCE in slow desorbing sites for 1, 3, or 30 days. Elution profiles were then measured to determine the extent of exchange that occurred while the columns were capped. Results from experiments conducted with different exchange times support the hypothesis that slow sorption kinetics is controlled by diffusion in micropores. For the silica gel and the Santa Clara sediment, ^{1}HTCE was incompletely exchanged with DTCE after 30 days (a time period that was sufficient for apparent equilibrium of a single sorbate). This indicates that the counter-diffusion rate of DTCE into ^{1}HTCE-filled micropores is less than the diffusion rate of ^{1}HTCE into micropores not filled with TCE.

Introduction

Risk-based corrective action (RBCA) guidelines are increasingly being used to define the scope of remediation at hazardous waste sites contaminated with volatile organic chemicals (VOCs) (*1*). Implementation of these guidelines can require predicting the extent of contamination under varying hydrogeologic, geologic, and environmental conditions. Such predictions require the use of mathematical models to define the transport and fate of VOCs in both space and time. One impediment to using such models is our inability to predict the effects of intraparticle mass transfer (i.e., sorption and desorption) on transport and degradation.

Sorption and desorption of VOCs in water wet geosorbents (e.g., soils and sediments) occur on two distinct time scales; a fast time scale occurring on the order of minutes to hours and a slow time scale occurring on the order of weeks to months (*2*−*6*). For the fast fraction, the pore diffusion model has been successfully used to predict trichloroethylene desorption from a range of well-characterized natural solids under both flow and no advective flow conditions (*7, 8*). Use of this model assumes that retarded diffusion through aqueous filled mesopores is the controlling mechanism.

For the slow fraction, recent evidence suggests that diffusion through hydrophobic micropore spaces controls VOC transport (*6*). Isotherm studies indicate that micropore spaces (or voids) may be formed from intraparticle mineral surfaces (*9, 10*) or condensed organic matter (*11*−*14*), where the latter may be formed from soil organic matter (*15, 16*) or combustion products such as soot and charcoal (*17*−*19*). In this study, we are not concerned with the origin of micropore spaces, only sorption and mass transfer properties within them.

To investigate these properties, the rate of exchange between deuterated trichloroethylene (DTCE) in fast desorbing sites and nondeuterated TCE (^{1}HTCE) in slow desorbing sites is examined for a silica gel, a Santa Clara sediment, and a Livermore clay/silt fraction, all at 100% relative humidity (RH) and 30 °C. In all previous sorption/desorption experiments conducted with natural soils and sediments, sorbate diffusion was unidirectional (i.e., either inward during adsorption or outward during desorption). By contrast, diffusion in the kinetic experiments reported here was counter-directional and is termed counter-diffusion. Results from these experiments will be used to test the hypotheses that in natural solids (i) slow desorption is controlled by diffusion through micropore spaces and (ii) counter-diffusion can be hindered by sorbate−sorbate interactions. The latter hypothesis has implications for predicting contaminant transport whenever chemical mixtures are present in the subsurface and different components of the mixture compete for the same slow sites.

Background

Mass Transfer. Previous investigators have shown that the slow sorption and desorption of VOCs are controlled by diffusion (as opposed to some other rate process such as first order) (*2, 5, 6, 20*). A diffusive process implies that rate-limiting transport occurs over a distance and that transport obeys Fick's second law:

$$\frac{\partial C_m}{\partial t} = D_m \frac{\partial^2 C_m}{\partial x^2} \tag{1}$$

where C_m is the concentration, t is the time, D_m is the diffusion coefficient, and x is the length variable. For slow desorption from uniformly contaminated identical sorption sites, the mass remaining can be described by the following analytical solution to eq 1 (*21*):

$$M_t = \frac{8M_{i,slow}}{\pi^2} \sum_{j=0}^{\infty} \frac{1}{(2j+1)^2} \exp\left(-\frac{D_m}{l_m^2}\frac{(2j+1)^2\pi^2 t}{4}\right) \tag{2}$$

where $M_{i,slow}$ is the initial slow desorbing mass and l_m is the distance over which diffusion occurs.

In many cases, a single diffusion rate constant (D_m/l_m^2) cannot describe diffusion from slow desorbing sites (*6*). Instead, a distribution of D_m/l_m^2 must be defined. To do this, eq 2 must be replaced by eq 3

$$M_{t,p(D_m/l_m^2)} = \int_{-\infty}^{\infty} p(D_m/l_m^2) M_t \mathrm{d}(D_m/l_m^2) \tag{3}$$

* To whom all correspondence should be addressed. Phone: (217)333-3822; fax: (217)333-6968; e-mail: werth@uiuc.edu.

† Present address: Department of Civil and Environmental Engineering, University of Illinois at Urbana−Champaign, Urbana, IL 61801.

10.1021/es9800378 CCC: $18.00
Published on Web 01/20/1999

where $p(D_m/l_m^2)$ is the probability density function. Prior work (*7*, *8*) has shown that the γ distribution, whose probability density function is shown in eq 4 (*22*), can be used to adequately describe the distribution of D_m/l_m^2 for the solids used in this study

$$p_{\alpha,\eta}(D_m/l_m^2) = \frac{\alpha^\eta (D_m/l_m^2)^{\eta-1} \exp(-\alpha D_m/l_m^2)}{\int_0^\infty \beta^{\eta-1} \exp(-\beta)\, d\beta} \quad (4)$$

where the denominator is the γ function, α is the scale parameter, η is the shape parameter, and the ratio of η to α is equal to the mean of the micropore diffusion rate constant ($\langle D_m/l_m^2 \rangle$). Equations 2−4 can be combined to obtain the mass remaining in slow desorbing sites characterized by a γ distribution of D_m/l_m^2 (*8*):

$$M_{t,p(D_m/l_m^2)} = \frac{8M_{i,slow}}{\pi^2} \sum_{j=0}^{\infty} \frac{1}{(2j+1)^2} \left(\frac{\eta}{\eta + (\langle D_m/l_m^2 \rangle)(2j+1)^2 \pi^2 t/4} \right)^\eta \quad (5)$$

In this paper, eq 2 will be referred to as the diffusion model (DM), and eq 5 will be referred to as the distributed diffusion model (DDM). The DM has two unknowns, $M_{i,slow}$ and D_m/l_m^2. The DDM has three unknowns, $M_{i,slow}$, $\langle D_m/l_m^2 \rangle$, and η. For large values of η, the DDM effectively reduces to the DM and $\langle D_m/l_m^2 \rangle = D_m/l_m^2$. For brevity, both D_m/l_m^2 and $\langle D_m/l_m^2 \rangle$ will hereafter be referred to as $\langle D_m/l_m^2 \rangle$.

Recent evidence suggests slow diffusive transport of VOCs in soils and sediments occurs in micropore spaces (*3*, *6*). Slow transport behavior in soil and sediment micropore spaces is expected to be similar to that in microporous zeolites. In zeolite ZSM-5, *p*-xylene sorption rates were found to decrease at high *p*-xylene concentrations (*23*). Isotherm measurements show a hysteresis loop in the adsorption/desorption isotherms for *p*-xylene in zeolite ZSM-5 (*23*−*25*). This was attributed to transformation of the *p*-xylene to a more stable, dense state at high concentrations. On the basis of these results, it was hypothesized that the uptake of *p*-xylene is reduced at high concentrations because diffusion occurs in a more dense arrangement of this sorbate (*23*).

Uptake rates of organics in zeolite micropores have also been related to the ratio of sorbate width to micropore width (*26*). As the sorbate width to micropore width increases, values of $\langle D_m/l_m^2 \rangle$ can decrease because the close proximity of sorbent walls obstructs diffusion of the sorbate (i.e., steric hindrance) and because forces of attraction between the sorbent walls and the sorbate increase. In geosorbents, a distribution of diffusion rate constants often describes slow desorption (*6*). Hence, there may be a distribution of micropore widths within these solids.

Similar to uptake rates, counter-diffusion rates in micropores may decrease as the sorbate width to micropore width increases. Decreasing pore widths in zeolite micropores can cause counter-diffusing molecules to obstruct each others movement (*27*). This phenomenon, also a form of steric hindrance, causes diffusion rates to be slow. Counter-diffusion rates in micropores may also be affected by competition for sorption sites when chemically different sorbates are present. McGinley et al. (*28*) observed that competing sorbates can displace each other and affect the time for a chemical to breakthrough a bed of sorbent. In this paper, we will evaluate the effects of counter-diffusion on uptake when both sorbates have an equal affinity for the sorbent (i.e., there is no competition for sorption sites).

Mesopore−Micropore Exchange and Elution. A simplified conceptual picture of the exchange and elution process occurring within a one-dimensional soil and sediment micropore is shown in Figure 1. This picture is based on three assumptions supported by previous work (*6*−*8*): (i) fast desorption from mesopores is instantaneous relative to slow desorption from micropores; (ii) micropore openings adjoin aqueous filled mesopores; and (iii) slow desorption is controlled by diffusion through hydrophobic micropore spaces.

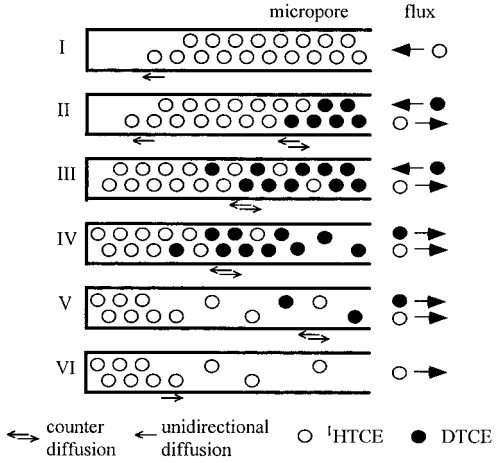

FIGURE 1. Conceptual exchange and elution of ^{1}HTCE and DTCE in a micropore. I, treatment of micropore with ^{1}HTCE. II, initial exchange of DTCE in mesopore with ^{1}HTCE in micropore. III, later time exchange of DTCE in mesopore with ^{1}HTCE in micropore. IV, initial elution of DTCE from micropore. V, later time elution of both ^{1}HTCE and DTCE from micropore. VI, later time elution of ^{1}HTCE from micropore.

The experimental approach first involves exposure of the solids packed within a column to ^{1}HTCE vapor. During an incubation period, ^{1}HTCE diffuses into hydrophobic micropores within the solids and either partially or, if time permits, completely fills them as shown in case I. Adsorption studies with zeolites show that water does not adsorb to an appreciable extent in hydrophobic micropores (*29*, *30*), presumably because it is energetically favorable for water molecules to remain hydrogen bonded in the liquid state (*30*). Hence, hydrophobic micropores are considered to contain air molecules (i.e., primarily N_2 and O_2) not water prior to incubation with ^{1}HTCE.

After incubation, the fast desorbing fraction of ^{1}HTCE is then rapidly replaced with DTCE. Based on previous work (*6*), replacing all of the ^{1}HTCE in the vapor phase of a column and in the aqueous filled mesopores of the solid with DTCE is complete within several minutes. Now, DTCE is allowed to exchange with ^{1}HTCE in slow desorbing sites. During exchange, DTCE diffuses into the micropores from the mesopores counter to the direction of ^{1}HTCE diffusion as shown in case II. If the ^{1}HTCE did not completely fill the micropores during incubation, ^{1}HTCE will also continue to diffuse further into the micropores. As time progresses, DTCE diffuses further into the micropores displacing the counter-diffusing ^{1}HTCE as shown in case III (note: if an infinite time was allowed to elapse, DTCE and ^{1}HTCE would be uniformly distributed throughout the micropores and mesopores according to their molar ratio).

After a specified exchange period, mass external to micropores is rapidly (i.e., minutes) removed by purging the column with water-saturated nitrogen gas. This creates a near-zero concentration boundary at micropore−mesopore interfaces. Now DTCE may diffuse both out of the micropores and deeper into the micropores (counter to the direction of ^{1}HTCE diffusion) at the same time. Since DTCE dominates the mass from the micropore entrance inward, the initial flux from micropores is primarily DTCE. Depending on how

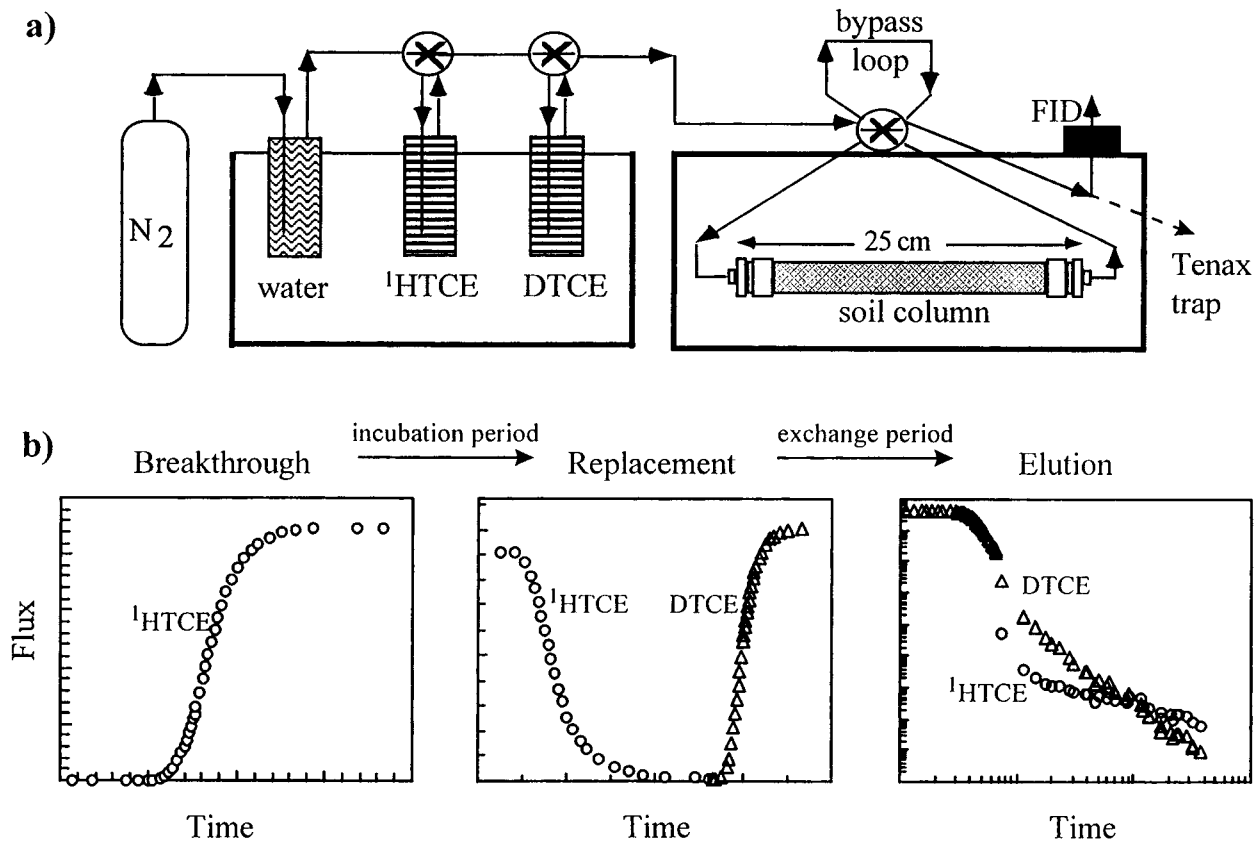

FIGURE 2. (a) Experimental setup for isotope exchange experiments. (b) Typical profiles obtained during breakthrough of ^{1}HTCE, replacement of ^{1}HTCE with DTCE in fast sites, and elution ^{1}HTCE and DTCE from slow sites.

deep DTCE penetrated the micropores, the mass remaining during this time may be comprised of mostly DTCE or ^{1}HTCE. If DTCE comprises the majority of mass remaining (i.e., greater than half of the mass in the micropores is DTCE), the mass of DTCE remaining will decrease first until more ^{1}HTCE remains in the micropores. Case IV illustrates the situation where there is an equal amount of ^{1}HTCE and DTCE remaining in the micropores.

When most of the DTCE has left the micropores, the fraction of ^{1}HTCE that makes up the flux increases and the fraction of DTCE that makes up the flux decreases. Since DTCE is loaded from the front end of micropores back, ^{1}HTCE will not dominate the flux until almost all of the DTCE has been removed. Case V illustrates the condition in the micropores when most of the DTCE has been removed and the flux is comprised of equal amounts of ^{1}HTCE and DTCE. After DTCE has diffused from the micropores, ^{1}HTCE will dominate the flux until all of the mass has diffused from the micropores (case VI).

Results presented here will be interpreted in the context of this simplified conceptual model. In reality, more complex geometries are possible and even likely. For instance, condensed organic matter may exist as isolated bodies within mineral aggregates. Micropore spaces formed from this material might be better represented by spherical matrixes of interconnected micropores. Alternatively, micropores might be better represented by funnel-shaped or undulating pores. Regardless of the geometry, ^{1}HTCE will still enter the micropore(s) first and come out last (and vice versa for DTCE) if the exchange of isotopically labeled TCE is controlled by mass transfer over a length scale. Thus, we believe that further consideration of more complex geometries would not augment data interpretation or change the conclusions reached in this paper.

Experimental Section

Sorbates and Sorbents. The only sorbates used in this study were ^{1}HTCE and DTCE. Properties of DTCE are assumed to be the same as those of ^{1}HTCE, except for molecular weight. TCE is a good model sorbate because it displays characteristics typical of many hydrophobic VOCs and is a common soil and groundwater contaminant (*31*−*33*). The DTCE (D, 98%) was purchased from Cambridge Isotope Laboratories. All DTCE fraction of flux values and all DTCE fraction of mass remaining values were increased by 2% to account for the impurity of the DTCE source.

Three sorbents were used in this study: a silica gel, a Santa Clara sediment, and a Livermore clay/silt fraction. Silica gel was used because it is considered to represent a model mineral solid containing both meso- and micropores. In previous studies, it has been shown to behave like natural soils and sediments with respect to both equilibria and kinetics (*3*, *6*, *9*, *10*). The Santa Clara sediment was used because this solid had the largest slow desorbing fraction of ^{1}HTCE of any solids examined in a previous study (*6*). The Livermore clay/silt was used because this solid had the lowest slow desorbing fraction of ^{1}HTCE of any solids examined in a previous study (*6*). Properties of these sorbents are listed elsewhere (*9*) and will be described in this paper as necessary.

Isotope Exchange Columns. The experimental setup and typical breakthrough, replacement, and elution profiles for the isotope exchange studies are shown in Figure 2. As described elsewhere, columns and fittings were all stainless steel, and columns were approximately 25 cm long (*10*). Assembled columns were filled with solids and equilibrated to 100% RH at 30 °C. As illustrated by the breakthrough profile in Figure 2b, the solids in the columns were then purged with nitrogen gas saturated with water and ^{1}HTCE until the effluent concentration, as measured by a flame-ionization detector (FID) mounted on a Hewlett-Packard (HP) 5890 gas

chromatograph (GC), appeared constant and equal to the influent concentration. At this point, the columns were capped and allowed to incubate. Incubation periods for the silica gel columns, the Santa Clara sediment columns, and the Livermore clay/silt fraction column were approximately 3, 1, and 1 week, respectively.

After incubation, the columns were purged with water-saturated nitrogen for 2−5 min to remove the fast desorbing fraction of ^{1}HTCE. The removal of this fraction of ^{1}HTCE was measured on-line with the FID and was represented by the declining portion of the replacement profile in Figure 2b. Immediately following this removal, a valve was switched and nitrogen gas saturated with water and DTCE was purged through the columns. This procedure replaced all of the fast desorbing ^{1}HTCE with DTCE. Once the effluent concentration equaled the influent concentration, columns were capped, and DTCE was allowed to exchange with ^{1}HTCE for either 1, 3, or 30 days.

After the exchange period, columns were purged with water-saturated nitrogen as illustrated by the elution profile in Figure 2b. Initially the effluent was measured on-line with the FID. During this time, the fast eluting fraction of contaminant was removed. Once column effluent dropped below the detection limit of the FID, it was trapped on a column of Tenax adsorbent for periods ranging from 1 min to 2 h depending on the effluent concentration. The trapped organic was then desorbed by heating the trap and releasing the effluent onto a GC equipped with an HP 5970 mass selective detector (MSD). By selecting one ion for the DTCE (132.39) and one ion for the ^{1}HTCE (131.39), it was possible to quantify the flux of ^{1}HTCE and the flux of DTCE eluting from columns during slow desorption. At the end of column purging, the remaining TCE was removed by heating the column up to 180 °C while trapping the eluted isotopes on Tenax traps and quantifying them with the MSD.

Mass balances were performed by comparing the total TCE sorbed (100% ^{1}HTCE) during initial breakthrough to the total TCE eluted (DTCE + ^{1}HTCE) during final desorption. During isotope exchange, DTCE was exchanged for ^{1}HTCE, so no net change in mass within the columns occurred. For all columns except the Livermore clay/silt, between 90% and 111% of the added mass was recovered. The mass balance for the Livermore clay/silt column was 68%. The mass loss in this column presumably occurred when it was uncapped and while being connected and disconnected from the purge apparatus (*9*).

To ensure that DTCE was not transforming to ^{1}HTCE during isotope exchange experiments, a column containing silica gel was contaminated with DTCE, incubated for approximately 1 month, eluted for 1 week, and then baked to remove the residual mass. No transformation of DTCE was observed during this process.

Model Application. For solids examined in this study, diffusion rate constants ($\langle D_m/l_m^2 \rangle$ and/or η) for DM or DDM profiles were obtained in previous studies (*6, 7*) by simulating the slow desorption of ^{1}HTCE from the same solid with no DTCE present. In the previous study, solids in all columns were at 100% RH, and columns were incubated for greater than 1 month with ^{1}HTCE before desorption profiles were measured. Values of $M_{i,slow}$ for these columns differed from those measured in this work (by up to 35% for silica gel and Santa Clara sediment and by 42% for Livermore clay/silt) because of variations in breakthrough times. Values of $M_{i,slow}$ in this study were adjusted to minimize the relative squared errors (*6, 34*) between model profiles and total mass remaining profiles (^{1}HTCE + DTCE) in the slow desorbing region. All diffusion rate constants and initial slow desorbing masses are documented in Table 1.

TABLE 1. Diffusion Rate Constants and Initial Slow Desorbing Masses

sorbent	$\langle D_m/l_m^2 \rangle$ (s^{-1})	η (−)	$M_{i,slow}$ (ppm)
silica gel	2.8×10^{-7} [a]	NA	19[b]
Santa Clara sediment	2.1×10^{-6} [c]	0.39	59[b]
Livermore clay/silt	2.8×10^{-5} [c]	0.39	4.3[d]

[a] Converted from the value obtained from a radial diffusion model simulation of slow desorbing ^{1}HTCE using $D_m/l_m^2 = 4.7(D_m/a^2)$ (*6*), where *a* is the radial diffusion length. Units for the radial diffusion rate constant value reported by Werth and Reinhard (*6*) were corrected from s^{-1} to min^{-1}. Value shown represents a single D_m/l_m^2 value. [b] Obtained by simulating the total mass remaining profile from a 3-day exchange time experiment. [c] Converted from a dimensionless model simulation of slow desorbing TCE with the same solid (*7*). Value shown represents the mean of the distribution of D_m/l_m^2 values. [d] Obtained by simulating the total mass remaining profile from a 1-day exchange time experiment.

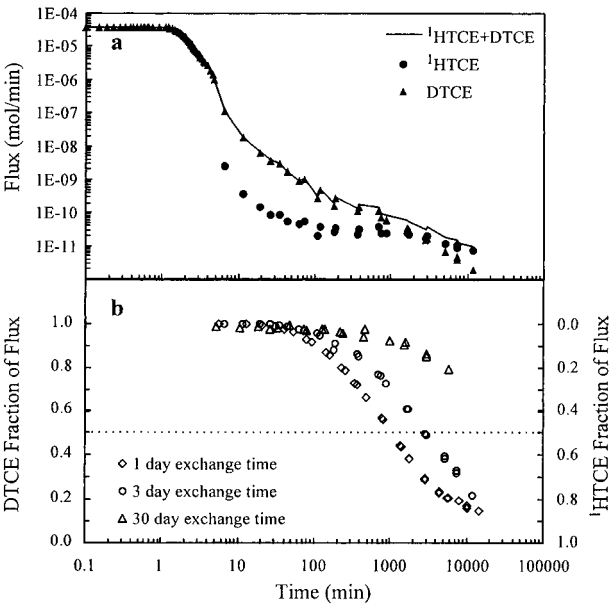

FIGURE 3. (a) Flux of ^{1}HTCE and DTCE from silica gel with a 3-day exchange time. (b) Fraction of flux of ^{1}HTCE and DTCE from silica gel with a 1-, 3-, and 30-day exchange time. Incubation time for all silica gel columns was approximately 3 weeks.

Results

Flux profiles for silica gel are shown in Figure 3. The transient flux of each TCE isotope for silica gel with a 3-day exchange time is shown in Figure 3a. On the basis of profile shape and previous modeling studies (*3, 4, 6*), fast desorption is complete in less than 10 min, and slow desorption begins after 10 min with the 'fast−slow' transition region in between. During fast desorption and much of slow desorption, the flux of DTCE coincides with the total flux (^{1}HTCE + DTCE) eluting from the column. At 2900 min, the flux profile for DTCE crosses the flux profile for ^{1}HTCE, causing the ^{1}HTCE flux to nearly coincide with the total flux after this time.

To illustrate the contribution of each TCE isotope to the total flux profile, the data in Figure 3a are plotted in Figure 3b as the ^{1}HTCE and DTCE fraction of the total flux. The fraction of flux profiles for silica gel with 1- and 30-day exchange times are also shown. The sum of the ^{1}HTCE fraction of the flux and the DTCE fraction of the flux always equals 1. Hence, a single profile with two corresponding ordinates (one for the ^{1}HTCE fraction of the flux and one for the DTCE fraction of the flux) is shown for each exchange time.

For all exchange times, the total flux is initially controlled by the flux of DTCE. A dotted line is drawn through the figure

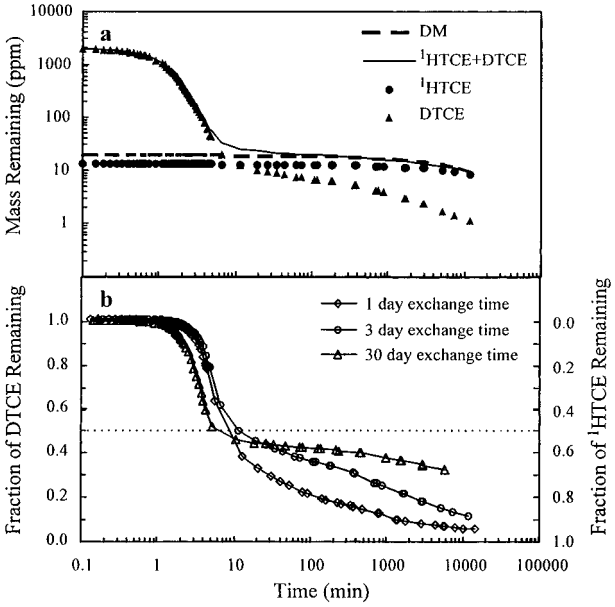

FIGURE 4. (a) Mass of ^{1}HTCE and DTCE remaining on silica gel with a 3-day exchange time and a DM profile of the total mass remaining. (b) Fraction of ^{1}HTCE and DTCE remaining on silica gel with a 1-, 3-, and 30-day exchange time. Incubation time for all silica gel columns was approximately 3 weeks.

at 0.5 (i.e., 50% line). This line is used as a reference to indicate the time when the total flux consists of equal amounts of DTCE and ^{1}HTCE. Before a profile crosses this line, DTCE controls the total flux. After a profile crosses this line, ^{1}HTCE controls the total flux. As shown, the time at which the fraction of flux profiles crosses the 50% line increases with increasing exchange time, indicating that with increasing exchange time a greater amount of DTCE exchanges with ^{1}HTCE in slow desorbing sites.

Experimental mass remaining profiles and a DM profile for silica gel are shown in Figure 4. In Figure 4a, the DTCE and ^{1}HTCE mass remaining profiles cross near 12 min; thereafter, the ^{1}HTCE remaining in the column exceeds the DTCE remaining, which gradually decreases to <1 ppm by 10 000 min. The slow desorbing region of the total mass remaining profile (^{1}HTCE + DTCE) and the shape of the ^{1}HTCE profile are well simulated by the DM profile.

To illustrate the contribution of each TCE isotope to the total mass remaining, the data in Figure 4a (and the 1- and 30-day exchange time data) are plotted in Figure 4b as the ^{1}HTCE and DTCE fraction of the total mass remaining. During the first few minutes the fraction of DTCE remaining is approximately 1. In the fast−slow transition region, the fraction of DTCE remaining in all three columns drops sharply, causing the profiles to cross the 50% line and the fraction of ^{1}HTCE remaining to exceed the fraction of DTCE remaining. Hence, the majority of the initial ^{1}HTCE in the slow desorbing sites was not displaced by the DTCE after 1-, 3-, or 30-day exchange times, suggesting that ^{1}HTCE deep within micropores did not exchange.

In Figure 4b, the fraction of mass remaining profiles for all three columns crosses the 50% line at or near the fast−slow transition region. In contrast, the fraction of flux profiles in Figure 3b crosses the 50% line in order of increasing exchange time. As documented in Table 2, the time at which the fraction of flux profiles crosses the 50% line is later than the time at which the fraction of mass remaining profiles crosses the 50% line for all three columns. This behavior is consistent with that expected for counter-diffusion in one-dimensional micropores, where DTCE in micropore openings dominates the total flux but not the total mass remaining in a column. Similarly, the fraction of mass remaining profiles crosses or approaches the 50% line before the fraction of flux profiles for all Santa Clara sediment and Livermore clay/silt columns (Figures5 and 6).

TABLE 2. Times When the Fraction of Flux and Mass Remaining Profiles Cross the 50% Line

sorbent	exchange time (days)	$^a t_{flux-cross}$ (min)	$^b t_{MR-cross}$ (min)
silica gel	1	1 100	9.4
	3	2 900	12
	30	>5 800	6.8
Santa Clara sediment	3	>43 000	10 000
	30	>53 000	30 000
Livermore clay/silt	1	>2 900	>2 900

[a] Time when the fraction of flux profile crosses the 50% line. [b] Time when the fraction of mass remaining profile crosses the 50% line.

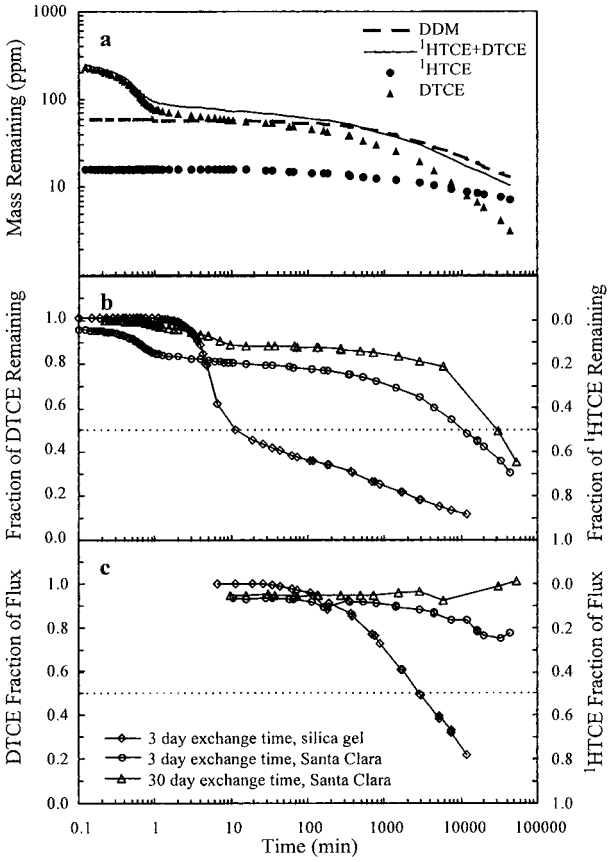

FIGURE 5. (a) Mass of ^{1}HTCE and DTCE remaining on Santa Clara sediment with a 3-day exchange time and a DDM profile of the total mass remaining. (b) Fraction of ^{1}HTCE and DTCE remaining on silica gel with a 3-day exchange time and on Santa Clara sediment with a 3- and 30-day exchange time. (c) Fraction of flux of ^{1}HTCE and DTCE from silica gel with a 3-day exchange time and from Santa Clara sediment with a 3- and 30-day exchange time. Incubation times for all silica gel columns and all Santa Clara sediment columns were approximately 3 and 1 week, respectively.

Mass remaining and flux profiles for Santa Clara sediment with 3- and 30-day exchange times are shown in Figure 5. For comparison, the fraction of mass remaining and flux profiles for silica gel with a 3-day exchange time are shown in Figure 5, panels b and c, respectively. In Figure 5a, the total mass remaining profile for the Santa Clara sediment with a 3-day exchange time coincides with the DDM profile. In contrast to the silica gel, the shape of the ^{1}HTCE remaining profile does not coincide with the shape of the DDM profile,

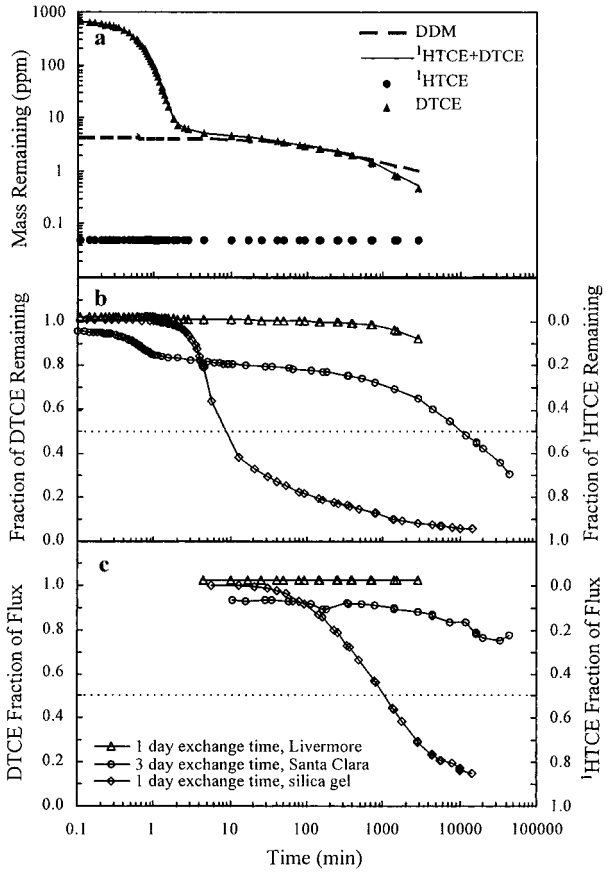

FIGURE 6. (a) Mass of [1]HTCE and DTCE remaining on the Livermore clay/silt fraction with a 1-day exchange time and a DDM profile of the total mass remaining. (b) Fraction of [1]HTCE and DTCE remaining on the Livermore clay/silt fraction and the silica gel with a 1-day exchange time and on the Santa Clara sediment with a 3-day exchange time. (c) Fraction of flux of [1]HTCE and DTCE from the Livermore clay/silt fraction and the silica gel with a 1-day exchange time and from the Santa Clara sediment with a 3-day exchange time. Incubation times for all silica gel columns, all Santa Clara sediment columns, and the Livermore clay/silt fraction column were approximately 3, 1, and 1 week, respectively.

indicating that the sum, but not the individual amounts, of [1]HTCE and DTCE behaves like [1]HTCE desorbing in the absence of DTCE. Since the analytical solution to the DDM is based on the assumption that mass is uniformly distributed within the micropore, the modeling results suggest that the sum, but not the individual amounts, of [1]HTCE and DTCE is uniformly distributed throughout the micropores.

In Figure 5b, the fraction of mass remaining profile for the Santa Clara sediment with a 30-day exchange time crosses the 50% line later than the corresponding profile for the Santa Clara sediment with a 3-day exchange time. Also, Santa Clara sediment profiles at both 3- and 30-day exchange times cross the 50% line much later than the fraction of mass remaining profile for silica gel with a 3-day exchange time. Since the silica gel profile with a 30-day exchange time crosses the 50% line within minutes of the time when the silica gel profile with a 3-day exchange time crosses the 50% line, a greater fraction of DTCE exchanges with [1]HTCE for the same exchange time in Santa Clara sediment than in the silica gel. This finding is consistent with results shown in Figure 5c. Here the fraction of flux profile for silica gel crosses the 50% line near 2900 min, while the fraction of flux profiles for the Santa Clara sediment does not cross the 50% line even after 43 000 min.

Mass remaining and flux profiles for the Livermore clay/silt fraction with a 1-day exchange time are shown in Figure 6. Fraction of mass remaining and flux profiles for Santa Clara sediment with a 3-day exchange time and for silica gel with a 1-day exchange time are also shown. In Figure 6a, the DTCE remaining in the Livermore clay/silt fraction exceeds the [1]HTCE remaining over the entire desorption profile, suggesting that DTCE exchanged deep within the micropores. The total mass remaining profile coincides with the DDM profile at early and intermediate times. However, at late times it appears that the total mass remaining profile starts to drop away from the DDM profile.

In Figure 6b, the fraction of mass remaining profile for the Livermore clay/silt fraction starts to curve downward near 2000 min. This is well after the corresponding profiles for silica gel cross the 50% line and after the corresponding profile for Santa Clara sediment starts to curve downward. Hence, exchange appears to be faster in the Livermore clay/silt fraction than in the silica gel or the Santa Clara sediment. Figure 6c supports this finding, where the DTCE fraction of flux for the Livermore clay/silt with a 1-day exchange time never drops below 1.

Discussion

Experimental and simulated mass remaining profiles for the silica gel and the Santa Clara sediment suggest that the sum, but not the individual amounts, of [1]HTCE and DTCE behaves like [1]HTCE desorbing in the absence of DTCE. This indicates that during counter-diffusion DTCE must exchange with [1]HTCE in a limited number of slow desorbing sites, causing the sum but not the individual components of [1]HTCE and DTCE to be uniformly distributed in the micropores. This conclusion may not apply to the Livermore clay/silt fraction, where the DDM profile begins to diverge from the total mass remaining profile at late times. This may be due to differences in incubation time between the column from which the apparent diffusion rate constant values were obtained (>1 month) and the isotope exchange column (1 week).

Agreement between the diffusion models and the total mass remaining profiles in silica gel and Santa Clara sediment supports an earlier finding that mass transfer in slow desorbing sites is controlled by diffusion. Two additional findings support this argument: (i) the extent to which DTCE exchanges with [1]HTCE in slow desorbing sites of silica gel and Santa Clara sediment increases with increasing exchange time and (ii) the time at which the fraction of the flux profiles for all three solids crosses or approaches the 50% line is later than the time at which the fraction of mass remaining profiles crosses or approaches this line.

Silica gel is engineered to contain pores of relatively uniform size and composition (*35*). Assuming uniform micropores as shown in Figure 1, DTCE is allowed to diffuse deeper into micropores with increasing exchange time, thus delaying the time at which the fraction of flux and mass remaining profiles crosses the 50% line. Also, since DTCE is assumed to displace [1]HTCE from the micropore entrance inward, the flux out of the micropore must initially be comprised of DTCE even if the majority of mass remaining is [1]HTCE. Similar behavior for the Santa Clara sediment and the Livermore clay/silt fraction suggests that diffusion controls transport in natural solid slow desorbing sites as well.

The extent of isotope exchange can be evaluated to determine if the rate of counter-diffusion is different than the rate of a single sorbate diffusing alone. In single sorbate experiments, Farrell and Reinhard (*3*) observed that incubation periods between 1and 3 months resulted in identical flux and mass remaining profiles during 1week of desorption for [1]HTCE from the solids used in this study. We also found no difference in 1-week flux and mass remaining profiles for [1]HTCE incubated with Santa Clara sediment for 1or 8 months

(data not shown). This indicates that 'apparent' equilibrium is achieved after TCE is exposed to a sorbent for less than 1 month.

During exchange, silica gel and Santa Clara sediment were exposed to DTCE for 30 days. If the rate of DTCE uptake during exchange is equal to the rate of ^{1}HTCE uptake in single sorbate experiments, the fraction of flux and mass remaining values for DTCE should remain constant and approximately equal to the initial values during the first week (i.e., 10 000 min) of elution. For silica gel with a 30-day exchange time, the fraction of flux and mass remaining for DTCE drops from 1 to 0.8 and 0.3, respectively, after 10 000 min of elution. Similarly, for the Santa Clara sediment with a 30-day exchange time, the fraction of DTCE remaining drops from 1 to 0.7 after 10 000 min of elution. These results suggest that diffusion of DTCE in the presence of ^{1}HTCE is slower than diffusion of ^{1}HTCE in the absence of a TCE isotope.

On the basis of sorbate behavior in zeolite micropores (*23*−*25*, *27*), we propose two possible mechanisms to account for the reduced uptake rates of DTCE during the exchange period. First, micropores are on the order of sorbate dimensions. Within these pores, DTCE and ^{1}HTCE obstruct each other when they move in opposite directions. This steric hindrance results in a decrease in the rate of diffusion. Second, TCE forms a more dense phase at high concentrations in micropores. When ^{1}HTCE diffuses into an empty micropore (i.e., filled only with air), this dense phase is not present until a pore is almost filled with ^{1}HTCE. However, when DTCE diffuses into a micropore filled with ^{1}HTCE, this dense phase is present during DTCE uptake and DTCE diffusion is hindered. Both of these mechanisms support the hypothesis that, within micropores, sorbate−sorbate interactions decrease the rate of counter-diffusion relative to the rate of a single sorbate diffusing alone.

Decreasing micropore width results in lower values of $\langle D_m/l_m^2 \rangle$ for desorption (*26*). From Table 1, values of $\langle D_m/l_m^2 \rangle$ decrease from the Livermore clay/silt fraction to the Santa Clara sediment to the silica gel. Decreasing micropore width can also result in greater sorbate−sorbate interactions (*27*) and, consequently, slower exchange rates. In this study, the extent of exchange decreased from the Livermore clay/silt fraction to the Santa Clara sediment to the silica gel. Hence, results from this study are consistent with those from previous studies (*6*, *7*), and they support the hypothesis that the mean micropore width decreases from the Livermore clay/silt fraction to the Santa Clara sediment to the silica gel.

Results presented here indicate that sorbate−sorbate interactions reduce the rate of counter-diffusion. In a previous study (*6*), different temperature desorption kinetic profiles for ^{1}HTCE from the same sorbents used here suggested that sorptive forces control desorption rates for individual sorbates. Hence, for sorbates with different sorption affinities, counter-diffusion may also be affected by competition for sorption sites within micropores. As a result, counter-diffusion rates for chemically different sorbates may deviate even more than observed here from diffusion rates for single sorbates alone. Predicting contaminant transport or bioavailability when mixtures of chemicals are present requires a more quantitative understanding of this complex process.

Acknowledgments

Support for this work was provided by Lawrence Livermore National Laboratory (LLNL) through B209039 and the Environmental Protection Agency through R822626-01-0. The authors thank Jun Li for reviewing an earlier version of this manuscript and three anonymous reviewers for their helpful comments. The content of this paper does not necessarily represent the views of the supporting organizations.

Literature Cited

(1) Begley, R. *Environ. Sci. Technol.* **1996**, *30*, 438A−441A.
(2) Ball, W. P.; Roberts, P. V. *Environ. Sci. Technol.* **1991**, *25*, 1237−1249.
(3) Farrell, J.; Reinhard, M. *Environ. Sci. Technol.* **1994**, *28*, 63−72.
(4) Grathwohl, P.; Reinhard, M. *Environ. Sci. Technol.* **1993**, *27*, 2360−2366.
(5) Pignatello, J. J. *Environ. Toxicol. Chem.* **1990**, *9*, 1117−1126.
(6) Werth, C. J.; Reinhard, M. *Environ. Sci. Technol.* **1997**, *31*, 697−703.
(7) Werth, C. J.; Cunningham, J.; Reinhard, M.; Roberts, P. V. *Water Resour. Res.* **1997**, *33*, 2727−2740.
(8) Cunningham, J.; Werth, C. J.; Roberts, P. V.; Reinhard, M. *Water Resour. Res.* **1997**, *33*, 2713−2726.
(9) Werth, C. J.; Reinhard, M. *Environ. Sci. Technol.* **1997**, *31*, 689−696.
(10) Farrell, J.; Reinhard, M. *Environ. Sci. Technol.* **1994**, *28*, 53−62.
(11) LeBoeuf, E. J.; Weber, W. J., Jr. *Environ. Sci. Technol.* **1997**, *31*, 1697−1702.
(12) De Jonge, H.; Mittelmeijer-Hazeleger, M. C. *Environ. Sci. Technol.* **1996**, *30*, 408−413.
(13) Xing, B.; Pignatello, J. J.; Gigliotti, B. *Environ. Sci. Technol.* **1996**, *30*, 2432−2440.
(14) Xing, B.; Pignatello, J. J. *Environ. Sci. Technol.* **1997**, *31*, 792−799.
(15) Grathwohl, P. *Environ. Sci. Technol.* **1990**, *24*, 1687−1693.
(16) Young, T. M.; Weber, W. J., Jr. *Environ. Sci. Technol.* **1995**, *29*, 92−97.
(17) Gustafsson, O.; Haghseta, F.; Chan, C.; MacFarlane, J.; Gschwend, P. *Environ. Sci. Technol.* **1997**, *31*, 203−209.
(18) Goldberg, E. D. *Black Carbon in the Environment*; John Wiley & Sons: New York, 1985.
(19) Chiou, C. T.; Kile, E. *Environ. Sci. Technol.* **1998**, *32*, 338−343.
(20) Steinberg, S. M.; Pignatello, J. J.; Sawhney, B. L. *Environ. Sci. Technol.* **1987**, *21*, 1201−1208.
(21) Crank, J. *The Mathematics of Diffusion*; Oxford University Press: New York, 1975.
(22) Pitman, J. *Probability*; Springer-Verlag: New York, 1993.
(23) Beschmann, K.; Kokotailo, G. T.; Riekert, L. *Chem. Eng. Process.* **1987**, *22*, 223−229.
(24) Olson, D. H.; Kokotailo, G. T.; Lawton, S. L.; Meier, W. M. *J. Phys. Chem.* **1981**, *85*, 2238−2243.
(25) Richards, R. E.; Rees, L. V. *Zeolites* **1988**, *8*, 35−39.
(26) Karger, J.; Ruthven, D. M. *Diffusion in Zeolites and Other Microporous Solids*; John Wiley & Sons: New York, 1992.
(27) Satterfield, C. N.; Cheng, C. S. *AIChE J.* **1972**, *18*, 724−728.
(28) McGinley, P. M.; Katz, L. E.; Weber, W. J., Jr. *Water Resour. Res.* **1996**, *32*, 3571−3577.
(29) Weitkamp, J.; Ernst, S.; Gunzel, B.; Deckwer, W.-D. *Zeolites* **1991**, *11*, 314−317.
(30) Flanigen, E. M.; Bennett, J. M.; Grose, R. W.; Cohen, J. P.; Patton, R. L.; Kirchner, R. M.; Smith, J. V. *Nature* **1978**, *271*, 512−516.
(31) Hirato, Y.; Nakasugi, O.; Yoshioka, M.; Sumi, K. *Water Sci. Technol.* **1992**, *25*, 9−16.
(32) Lesage, S.; Jackson, R. E.; Priddle, M. W.; Riemann, P. G. *Environ. Sci. Technol.* **1990**, *24*, 559−566.
(33) Olivieri, A. W.; Eisenberg, D. M.; Kurtovich, M. R.; Pettegrew, L. *J. Water Resour. Plan. Manage.* **1985**, *111*, 346−358.
(34) Saez, P. B.; Rittmann, B. E. *Water Res.* **1992**, *26*, 789−796.
(35) Scott, R. P. W. *Silica Gel and Bonded Phases*; John Wiley & Sons: New York, 1993.

Received for review January 15, 1998. Revised manuscript received December 2, 1998. Accepted December 4, 1998.

ES9800378